Article

Comparative Analysis of Skeletal Muscle Metabolites of Fish with Various Rates of Aging

Dmitry L. Maslov *, Oxana P. Trifonova, Anton N. Mikhailov, Konstantin V. Zolotarev, Kirill V. Nakhod, Valeriya I. Nakhod, Nataliya F. Belyaeva, Marina V. Mikhailova, Petr G. Lokhov and Alexander I. Archakov

Institute of Biomedical Chemistry, 10 building 8, Pogodinskaya street, Moscow 119121, Russia; oxana.trifonova@gmail.com (O.P.T.); myhas84@mail.ru (A.N.M.); fireaxe@mail.ru (K.V.Z.); g-s2011@mail.ru (K.V.N.); kardavaleriya@yandex.ru (V.I.N.); natalia.belyaeva@ibmc.msk.ru (N.F.B.); m_mikhailova@mail.ru (M.V.M.); lokhovpg@rambler.ru (P.G.L.); alexander.archakov@ibmc.msk.ru (A.I.A.)

* Correspondence: dlmaslov@mail.ru; Tel.: +7-499-246-6980

Abstract: Fish species exhibit great diversity rating of aging (from negligible to rapid), which gives a unique possibility for the discovery of the molecular mechanisms that determine the differences in the rate of aging. A mass spectrometric metabolic profiling of skeletal muscle of fish with various aging rates was carried out by direct injection to a quadrupole time-of-flight mass spectrometer. The first group includes long-lived fish species (pike (*Esox Lucius*) and sterlet (*Acipenser ruthenus*); the second group—species with gradual senescence such as that observed in many mammalian species of similar size (zander (*Sandra lucioperca*) and perch (*Perca fluviatilis*)) and the third group—species with very short life cycle (chum salmon (*Oncorhynchus keta*) and pink salmon (*Oncorhynchus gorbuscha*)). Multivariate analysis of metabolic profiles allowed the detecting of about 80 group-specific features associated with amino acids, lipids, biogenic amines, intermediates of glycolysis, glycogenolysis, and citric acid cycle. Possible roles in the aging process are hypothesized for the biochemical pathways of the metabolites that were altered in the different groups.

Keywords: aging; metabolome profiling; muscle; fish

1. Introduction

A great range of ages is observed among different animals, including various species of fish. Some fish species (rockfish, sturgeon) has not revealed any age-related decline in their physiological capacity (including reproduction) for several decades of observation. The life cycle of other species (*genus nothobranchius*) is very short and does not exceed several weeks even in protected environments [1,2]. During the investigation of the aging process in animals, C. Finch has proposed to divide organisms into three categories differing in the rate of aging: negligible (long-lived species), gradual (species whose aging rate is similar to mammal species), and rapid (species with very short life cycle) [3]. According to the Finch's criteria, the main signs of negligible aging are continuous growth (although slow in most cases), the absence of an age-related increase in mortality rate, the absence of a decline in physiological capacity (including reproductive capacity) and disease resistance [3]. Sterlet, as well as flatfish, beluga, and rockfish, were classified as species with negligible aging [4]. Pike (*Esox Lucius*) can also be attributed to the same group [5]. Such species as guppy, red panchax, medaka, platyfish, Indian murrel, zander, and perch exhibit gradual senescence, which is typical for most vertebrates [4,6]. The age-related decline of regenerative ability, increasing the probability of physiological damages with advancing age, is an attribute of these species [5].

Finally, the last group (rapid aging) is characterized by rapid senescence with more or less synchronous deterioration of physiological capacity of all organs of an organism. Such species often die after spawning. Lampreys, eels, and Pacific salmonids may be included in this category.

The observable diversity in the lifespan among fish species provides an opportunity for the investigation of mechanisms responsible for dramatic differences in the rate of aging [7]. The long-lived species (negligibly senescent) may be considered as original antiaging models. Investigation of these species may facilitate determination of the pathways that protect effectively against the degenerative process. On the contrary, rapidly senescent species may be considered as models of accelerated aging. Comprehensive research of the species can help identify mechanisms associated with the fast development of age-related pathologies [8,9].

A progressive decrease of muscle mass and strength leading to deterioration of physiological functions of an organism, as well as the development of age-related disorders are one of the most notable factors of aging [10]. Skeletal muscles play a key role in the maintenance of healthy and active lifestyle since they are involved in many essential functions: control of movement and pose, physical function, participation in metabolism (for example, skeletal muscles are critical for the maintenance of glycaemic level), etc. [11–13]. Unfortunately, our knowledge about the pathophysiology of the loss of muscle mass and strength is still limited [14].

A metabolomics-based investigation of the skeletal muscle of the three fish groups with different aging rate was performed: the first group consists of biosamples of negligibly senescent species (pike (*Esox lucius*) and sterlet (*Acipenser ruthenus*), the second group—biosamples of gradually senescent species (zander (*Sander lucioperca*) and perch (*Perca fluviatilis*), and the third one includes biosamples of rapidly senescent species (chum salmon (*Oncorhynchus keta*), and pink salmon (*Oncorhynchus gorbuscha*). Comparative analysis of untargeted metabolomics data allows detecting the group-specific features. Subsequent analysis of the selected features enables the removal of artifacts, identify metabolites and detect pathways, in which the metabolites may be involved. An investigation of the contribution of these pathways to the functioning of the organism may provide insights into biological mechanisms related to the processes of maintenance of muscle mass and development of degenerative process [15].

2. Results

The method of Direct-Injection Electrospray Ionization Mass Spectrometry (DI-ESI-MS) was used in the study. An application of an untargeted approach enabled the detection of about 4000 different m/z ions. Multivariate analysis of metabolic data was performed after normalization and the removal of artifacts and outliers. Metabolite ions that were found at least in 70% of samples in each of the compared groups were admitted to the analysis. Principal component analysis of mass spectrometry spectra allowed validating the presence of significant differences in metabolic composition between samples related to different groups (Figure 1). A Kruskal-Wallis H test reconfirmed the results and enabled to detect features, the intensity of which was significantly different ($p < 0.05$) in the compared groups. It should be noted that no significant gender differences in the metabolic profiles were revealed (data not shown).

About 80 statistical significant features ($p < 0.05$) were detected by the comparative analysis. Results of the putative identification of the features showed that they are amino acids, biogenic amines, carnitines, intermediates of glycolysis, glycogenolysis, citric acid cycle, and lipid metabolism (Table 1). The identification of the metabolites was carried out by using two orthogonal characteristics (accurate mass and isotopic abundance distribution) that satisfy level 2 (putatively annotated compounds) according to the Metabolomics Standards Initiative (MSI) requirements (http://www.metabolomics-msi.org/). It should be noted that some masses were redundant—they have several candidates. The candidates have identical brutto-formula and, consequently, identical isotope distribution that does not permit proper differentiating by the method of metabolite identification applied in this study. However, these candidates belong to the same compound classes that meet the level 3 of metabolite identification (putatively annotated compound classes) [16]. The further consideration

of such metabolites represented the authors' point of view based on previously published results of identification.
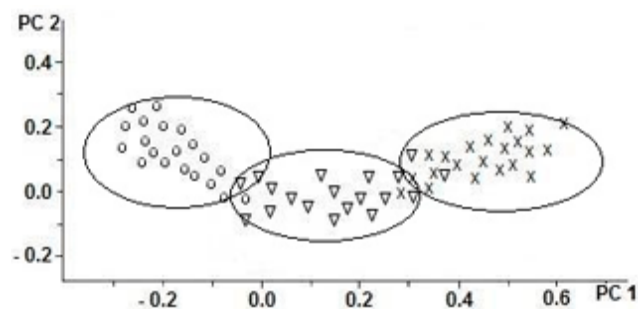

Figure 1. The Principal Component Analysis (PCA) score plot of mass spectrometry spectra illustrates the clustering of samples according to attributed group membership (negligible (×), gradual (Δ), and rapid aging (O)), with more than 80% of total variance (the first two components). The clustering displays a difference in the metabolic composition between the compared groups.

For more specific identification, a tandem mass spectrometry (MS/MS) method was applied. Metabolites of great biological significance (observed mainly in the samples related to negligible and gradual senescence) and whose concentration exceeded the limits of the method were selected for the analysis. Figure 2 shows the fragment list resulting from MS/MS fragmentation of selected metabolite (m/z—162,1150).
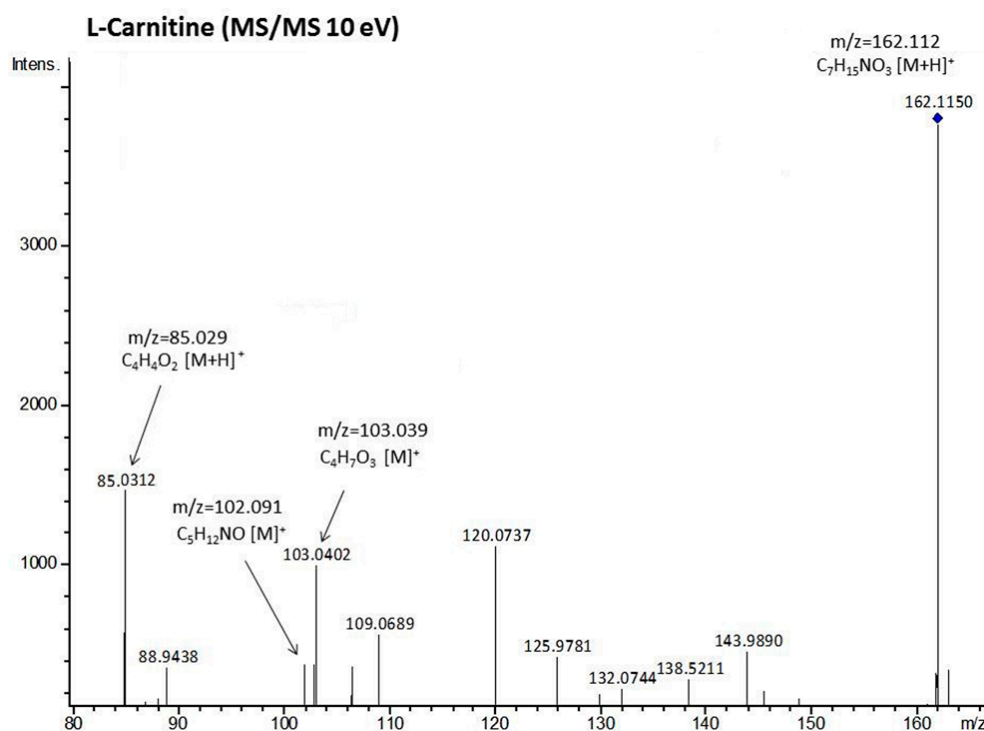

Figure 2. The results of tandem mass spectrometry (MS/MS) fragmentation of selected metabolites (m/z—162,1150). MS/MS spectra obtained in positive ionization mode. Collision energy—10 eV. Reference m/z value of fragments of l-carnitine, chemical formula and ion type (taken from the public metabolite database) are also indicated in the figure.

Figure 3 shows fragment list resulting from MS/MS fragmentation of selected metabolites (m/z—132,0777 and m/z—132,1024).

Table 1. Distinctive *m/z* features and putatively identified skeletal muscle metabolites typical for fish species with different lifespan.

			Mass of Ion				
Nº	Metabolite	HMDB ID	Measured (*m/z*)	Calculated (*m/z*)	Monoisotopic Mol Weight (Da)	Ion Form	Elemental Composition
			metabolites a high level of which was observed in the samples relating to negligible				
1	hypotaurine	HMDB00965	110,0175	110,027	110,0275	M+H	$C_2H_7NO_2S$
2	creatinine	HMDB00562	114,0634	114,0661	113,0589	M+H	$C_4H_7N_3O$
3	creatinine	HMDB00562	136,0027	136,0481	113,0589	M+Na	$C_4H_7N_3O$
4	L-carnitine	HMDB00062	162,1123	162,1124	161,10519	M+H	$C_7H_{15}NO_3$
5	n/a	—	635,3064	—	—	—	—
6	PC *	HMDB08531	844,6487	844,679	843,6717	M+H	$C_{48}H_{94}NO_8P$
			metabolites a high level of which was observed in the samples relating to negligible and gradual				
7	alanine	HMDB00161	90,0518	90,0549	89,04767	M+H	$C_3H_7NO_2$
8	alanine	HMDB00161	112,0307	112,0368	89,04767	M+Na	$C_3H_7NO_2$
9	valine	HMDB00883	118,0851	118,0862	117,0789	M+H	$C_5H_{11}NO_2$
10	sarcosine	HMDB00271	128,0106	128,0108	89,04767	M+K	$C_3H_7NO_2$
11	taurine	HMDB00251	126,0186	126,0219	125,0146	M+H	$C_2H_7NO_3S$
12	creatine	HMDB00064	132,0764	132,0767	131,0694	M+H	$C_4H_9N_3O_2$
13	leucine	HMDB00687	132,1024	132,1019	131,0946	M+H	$C_6H_{13}NO_2$
14	valine	HMDB00883	140,0617	140,0681	117,0789	M+Na	$C_5H_{11}NO_2$
15	taurine	HMDB00251	147,9842	148,0038	125,0146	M+Na	$C_2H_7NO_3S$
16	creatine	HMDB00064	154,0571	154,0586	131,0694	M+Na	$C_4H_9N_3O_2$
17	spermidine	HMDB01257	146,1466	146,1651	145,1578	M+H	$C_7H_{19}N_3$
18	maleylacetate	HMDB60348	159,0280	159,0288	158,0215	M+H	$C_6H_6O_5$
19	leucine	HMDB00687	170,0253	170,0577	131,0946	M+K	$C_6H_{13}NO_2$
20	maleylacetate	HMDB60348	196,9787	196,9847	158,0215	M+K	$C_6H_6O_5$
21	n/a	—	713,4983	—	—	—	—

Table 1. *Cont.*

Nº	Metabolite	HMDB ID	Mass of Ion		Monoisotopic Mol Weight (Da)	Ion Form	Elemental Composition
			Measured (*m/z*)	Calculated (*m/z*)			
metabolites a high level of which was observed in the samples relating to gradual						
22	itaconic acid	HMDB02092	152,9764	153,0158	130,0266	M+Na	$C_5H_6O_4$
23	n/a	—	771,6006	—	—	—	—
24	PC *	HMDB08136	802,5179	802,5357	779,5465	M+Na	$C_{44}H_{78}NO_8P$
25	PC *	HMDB08138	804,5363	804,5513	781,5621	M+Na	$C_{44}H_{80}NO_8P$
26	PC *	HMDB08136	822,5332	822,5410	783,5778	M+K	$C_{44}H_{82}NO_8P$
27	PC *	HMDB08589	826,6635	826,6684	825,6611	M+H	$C_{48}H_{92}NO_7P$
28	PC *	HMDB08304	832,5702	832,5827	809,5934	M+Na	$C_{46}H_{84}NO_8P$
29	PC *	HMDB08272	834,5845	834,5983	811,6091	M+Na	$C_{46}H_{86}NO_8P$
30	PC *	HMDB08467	844,5150	844,5253	805,5621	M+K	$C_{46}H_{80}NO_8P$
metabolites a high level of which was observed in the samples relating to rapid						
31	n/a	—	100,1074	—	—	—	—
32	serine	HMDB00187	106,0391	106,0498	105,0425	M+H	$C_3H_7NO_3$
33	pyruvate	HMDB00243	110,996	111,0053	88,01604	M+Na	$C_3H_4O_3$
34	lactic acid	HMDB00190	113,0268	113,0209	90,03169	M+Na	$C_3H_6O_3$
35	cysteine	HMDB00574	122,0211	122,0270	121,0197	M+H	$C_3H_7NO_2S$
36	choline	HMDB00097	127,0841	127,0967	104,1075	M+Na	$C_5H_{14}NO$
37	lactic acid	HMDB00190	128,9881	128,9948	90,03169	M+K	$C_3H_6O_3$
38	n/a	—	137,1283	—	—	—	—
39	fumaric acid	HMDB00134	138,9945	139,0002	116,0109	M+Na	$C_4H_4O_4$
40	niacinamide	HMDB01406	145,0250	145,0372	122,048	M+Na	$C_6H_6N_2O$
41	malate	HMDB00156	156,998	157,0107	134,0215	M+Na	$C_4H_6O_5$
42	α-ketoglutarate	HMDB00208	168,9989	169,0107	146,0215	M+Na	$C_5H_6O_5$

Table 1. *Cont.*

Nº	Metabolite	HMDB ID	Measured (*m/z*)	Calculated (*m/z*)	Monoisotopic Mol Weight (Da)	Ion Form	Elemental Composition
				Mass of Ion			
43	serinyl-alanine	HMDB29032	177,0656	177,0869	176,0797	M+H	$C_6H_{12}N_2O_4$
44	methylenesuccinic acid	HMDB59762	180,9791	180,9898	142,0266	M+K	$C_6H_6O_4$
45	α-ketoglutarate	HMDB00208	184,9788	184,9846	146,0215	M+K	$C_5H_6O_5$
46	threoninyl-alanine	HMDB29054	191,0972	191,1026	190,0953	M+H	$C_7H_{14}N_2O_4$
47	serinyl-alanine	HMDB29032	190,0210	190,0689	176,0797	M+Na	$C_6H_{12}N_2O_4$
48	citric acid	HMDB00094	215,0120	215,0162	192,0270	M+Na	$C_6H_8O_7$
49	n/a	—	227,1875	—	—	—	—
50	tridecanoic acid	HMDB00910	237,1446	237,1825	214,1932	M+Na	$C_{13}H_{26}O_2$
51	palmitoleic acid	HMDB03229	279,2001	279,2294	256,2402	M+Na	$C_{16}H_{30}O_2$
52	n/a	—	285,2529	—	—	—	—
53	linolenic acid	HMDB013	301,1796	301,2138	278,2245	M+Na	$C_{18}H_{30}O_2$
54	linoleic acid	HMDB00673	303,2024	303,2294	280,2402	M+Na	$C_{18}H_{32}O_2$
55	oleic acid	HMDB020	305,2036	305,2451	282,2558	M+Na	$C_{18}H_{34}O_2$
56	linolenic acid	HMDB013	317,1567	317,1877	278,2245	M+K	$C_{18}H_{30}O_2$
57	linoleic acid	HMDB00673	319,1922	319,2033	280,2402	M+K	$C_{18}H_{32}O_2$
58	eicosapentaenoic acid	HMDB01999	325,2039	325,2138	302,2245	M+Na	$C_{20}H_{30}O_2$
59	eicosapentaenoic acid	HMDB01999	341,1619	341,1877	302,2245	M+K	$C_{20}H_{30}O_2$
60	eicosadienoic acid	HMDB05060	347,2045	347,2346	308,2715	M+K	$C_{20}H_{36}O_2$
61	docosahexaenoic acid	HMDB00021	351,2073	351,2294	328,2402	M+Na	$C_{22}H_{32}O_2$
62	docosatrienoic acid	HMDB02823	357,2388	357,2764	334,2871	M+Na	$C_{22}H_{38}O_2$
63	d-maltose	HMDB00163	365,0830	365,1054	342,1162	M+Na	$C_{12}H_{22}O_{11}$
64	MG *	HMDB11539	375,2064	375,2505	352,2613	M+Na	$C_{21}H_{36}O_4$
65	MG *	HMDB00115	379,2473	379,2818	356,2926	M+Na	$C_{21}H_{40}O_4$
66	tetradecenoylcarnitine	HMDB02014	392,2518	392,2771	369,2879	M+Na	$C_{21}H_{39}NO_4$

Table 1. *Cont.*

Nº	Metabolite	HMDB ID	Mass of Ion			Ion Form	Elemental Composition
			Measured (*m/z*)	Calculated (*m/z*)	Monoisotopic Mol Weight (Da)		
67	MG *	HMDB11547	419,2218	419,2558	380,2926	M+K	$C_{23}H_{40}O_4$
68	hydroxycholesterol	HMDB02103	425,3057	425,339	402,3497	M+Na	$C_{27}H_{46}O_2$
69	MG *	HMDB11551	437,3341	437,3601	414,3709	M+Na	$C_{25}H_{50}O_4$
70	LPA *	HMDB07854	439,2501	439,2819	438,2746	M+H	$C_{21}H_{43}O_7P$
71	n/a	—	445,0474	—	—	—	—
72	PA *	HMDB11144	447,2502	447,2845	424,2953	M+Na	$C_{21}H_{45}O_6P$
73	LPA *	HMDB07855	459,2192	459,2482	436,2589	M+Na	$C_{21}H_{41}O_7P$
74	LysoPC *	HMDB10379	468,2750	468,3084	467,3011	M+H	$C_{22}H_{46}NO_7P$
75	LysoPC *	HMDB10383	494,3033	494,3241	493,3168	M+H	$C_{24}H_{48}NO_7P$
76	n/a	—	538,4796	—	—	—	—
77	n/a	—	551,3859	—	—	—	—
78	DG *	HMDB56009	591,4606	591,4959	568,5066	M+Na	$C_{35}H_{68}O_5$
79	DG *	HMDB56010	619,4817	619,5272	596,5379	M+Na	$C_{37}H_{72}O_5$
80	n/a	—	647,3752	—	—	—	—
81	DG *	HMDB56204	655,4883	655,5272	632,5379	M+Na	$C_{40}H_{72}O_5$
82	DG *	HMDB56298	663,4551	663,4959	640,5066	M+Na	$C_{41}H_{68}O_5$
83	DG *	HMDB56037	675,5749	675,5898	652,6005	M+Na	$C_{41}H_{80}O_5$
84	DG *	HMDB07430	693,4931	693,5428	670,5536	M+Na	$C_{43}H_{74}O_5$
85	PC *	HMDB08519	892,6545	892,6790	891,6717	M+H	$C_{52}H_{94}NO_8P$

Metabolites were annotated by library search (HMDB), accurate mass and isotopic abundance distribution; *m/z*—mass-to-charge ratio; n/a—not assigned; DG—diacylglycerol; MG—monoacylglycerol; LPA—lysophosphatidic acid; PA—phosphatidic acid; LysoPC –lysophospholipid; PC—phosphatidylcholine; *—redundant masses with several candidates.
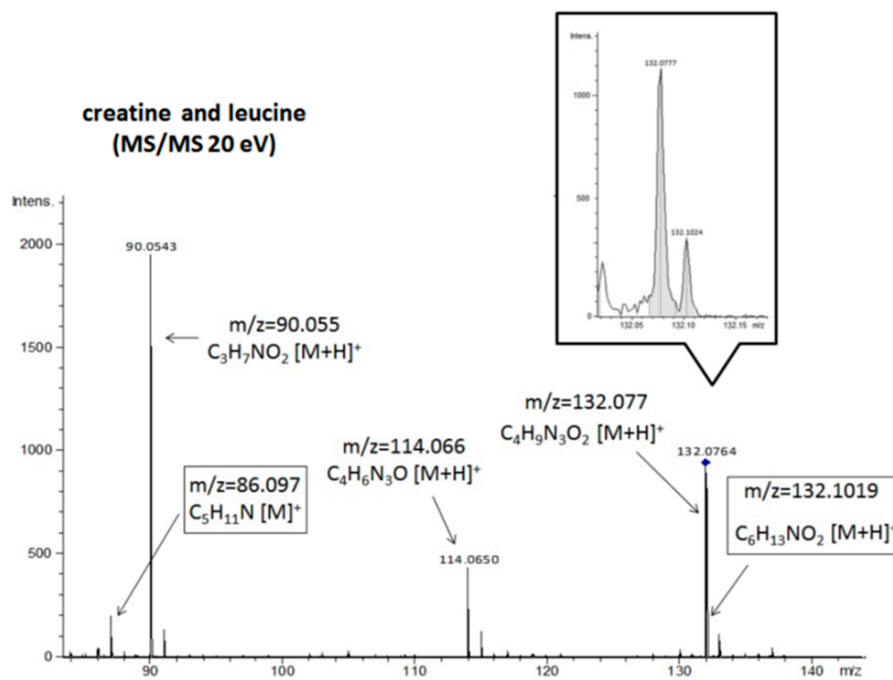
Figure 3. The results of MS/MS fragmentation of selected metabolites (*m/z*—132,0777 and *m/z*—132,1024). MS/MS spectra obtained in positive ionization mode. Collision energy—20 eV. Reference *m/z* value of fragments of leucine, creatine, chemical formula and ion type (taken from the public metabolite database) are also indicated in the figure.

Results of metabolites identification using MS/MS analysis are summarized in Table 2.

Table 2. Identification of selected metabolites by MS/MS fragmentation.

Metabolite	Precursor Ion				Product Ion			
	Registered *m/z*, Da	Calculated *m/z*, Da	Chemical Formula	Ion Type	Registered *m/z*, Da	Reference *m/z*, Da	Chemical Formula	Ion Type
leucine	132,1024	132,1019	$C_6H_{13}NO_2$	$[M + H]^+$	86,097	86,0969 *	$C_5H_{11}N$	$[M]^+$
					—	44,0499 *	C_2H_5N	$[M + H]^+$
					—	43,0546 *	C_3H_6	$[M + H]^+$
creatine	132,0777	132,0764	$C_4H_9N_3O_2$	$[M + H]^+$	114,065	114,0664 *	$C_4H_6N_3O$	$[M + H]^+$
					90,0543	90,0552 *	$C_3H_7NO_2$	$[M + H]^+$
L-carnitine	162,1126	162,1125	$C_7H_{15}NO_3$	$[M + H]^+$	103,0402	103,039 *	$C_4H_7O_3$	$[M]^+$
					102,0914	102,0913 *	$C_5H_{12}NO$	$[M]^+$
					85,0312	85,0284 *	$C_4H_4O_2$	$[M + H]^+$

Identification was performed by comparing detected *m/z* values of fragments (resulting from MS/MS fragmentation of selected metabolites) to corresponding *m/z* value of the reference fragments of leucine, creatine, and l-carnitine from the public metabolite database; *m/z*—mass-to-charge ratio. A mass tolerance window—0,005 Da. *—the reference results of MS/MS fragmentation were taken from public metabolite database METLIN.

Thus the results of MS/MS fragmentation confirmed the results of the earlier identification.

The distribution of the relative intensity of the putative metabolites in the compared groups is demonstrated in Figure 4. Careful examination of selected metabolites allowed dividing the major part of them into several groups. The first group may be named as the "group of amino acids". A high level of some amino acids (valine, leucine, alanine, taurine, and hypotaurine) was observed in the samples related to negligible senescence (Figure 4 metabolites 1, 8, 11, 13, and 14). However, a high level of some of these metabolites was also registered in the samples related to gradual senescence. The second group is the "group of biogenic amines". A high level of spermidine was observed in the samples related to negligible senescence (Figure 4 metabolite 17). The third group of metabolites may

be named as the "group of energy metabolism". Creatine, creatinine, carnitines, and the intermediates of the citric acid cycle may be associated with the group. A high level of creatine, creatinine, and L-carnitine is noted in the samples related to negligible senescence (Figure 4 metabolites 3, 4, 12), while the accumulation of medium and long-chain acylcarnitines and the intermediates of the citric acid cycle (fumarate, malate, alpha-ketoglutarate, and citrate) is observed in the samples related to rapid senescence (Figure 4 metabolites 39, 41, 42 48). The fourth group may be named as the "group of intermediates of sugar metabolism". There was an accumulation of the intermediates of sugar metabolism (maltose, lactate, and pyruvate) in the samples related to rapid senescence (Figure 4 metabolites 33, 34, 63). Finally, the fifth group is the "group of lipid metabolism". A high level of various lipid intermediates was observed in the samples related to rapid senescence.
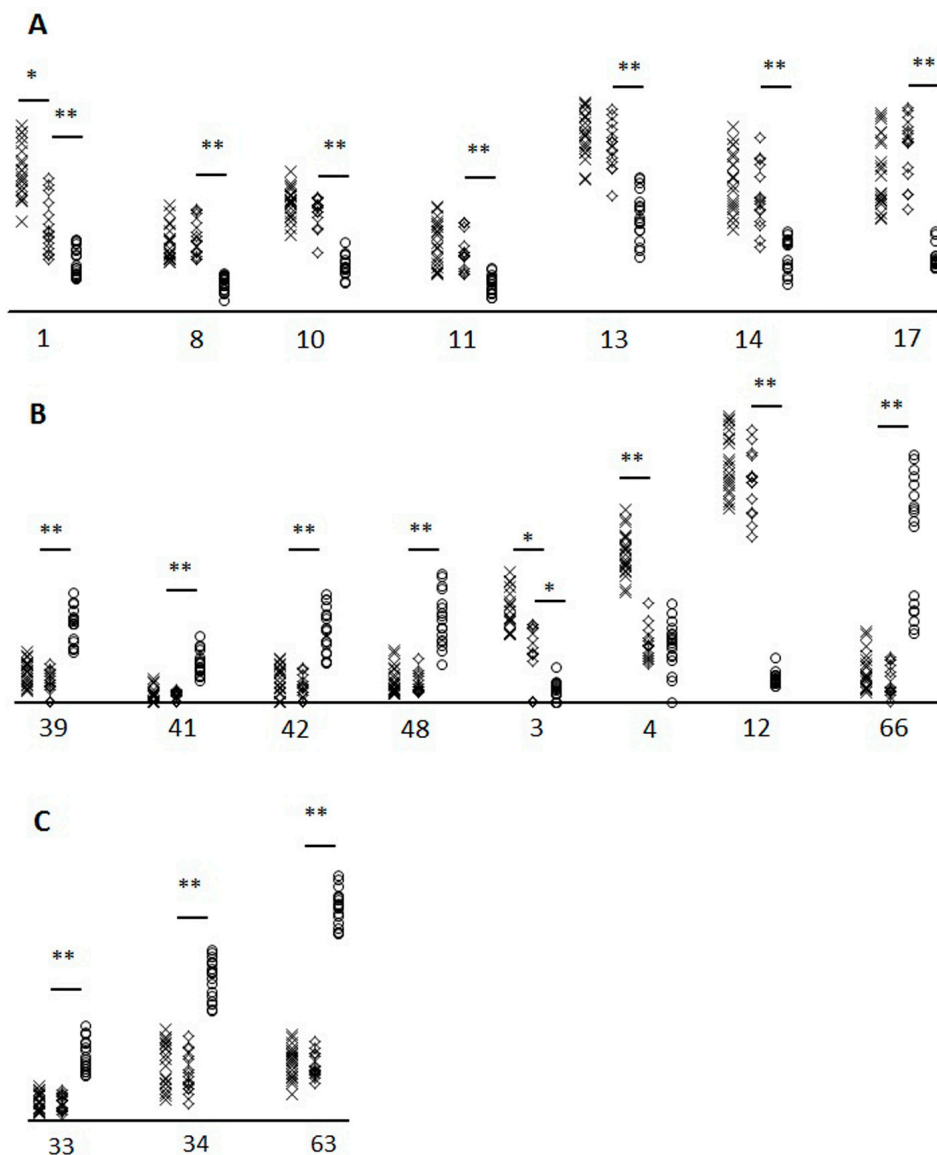
Figure 4. Results of the univariate statistical analysis identified metabolites with statistically significant differences among groups (negligible—(×), gradual—(◊) and rapid senescence—(O)). A.-metabolites related to a "group of amino acids" and a "group of biogenic amines" (alanine, valine, leucine, taurine, hypotaurine, and spermidine); B.-metabolites related to a "group of energy metabolism" (creatine, creatinine, carnitines, fumarate, malate, alpha-ketoglutarate, and citrate); C.-metabolites related to a "group of intermediates of sugar metabolism" (maltose, lactate, and pyruvate). The scatter plots show the intensity (relative units) of identified metabolites in the three compared groups. (**—$p < 0.01$; *—$p < 0.05$). Numbers are corresponded to ordinal metabolites numbers indicated in Table 1.

3. Discussion

A method of comparative analysis is one of the universal approaches for the detection and identification of key components that are a source of heterogeneity between samples [17]. Fish are the ideal model for investigations of the biochemical basis of the aging process by the approach. The availability of a large number of similar physiological, biochemical, and histological characteristics between fish species enables one to minimize the list of features which should be analyzed to identify metabolites and pathways that are possibly associated with the aging process. Availability of a lot of fish species belonging to different types of aging enable to include several species in each analyzed group allowing to eliminate a various species-specific metabolic perturbations (only group-specific perturbations should be selected for subsequent analysis).

An opportunity to perform large-scale experiments is another one advantage of the experimental model with fish. Most of the fish organs (heart, excretory organs, digestive organs, etc.) are analogous to organs of other vertebrates [18]. This fact provides the possibility of translating the results onto processes in mammals. This study is a follow-up to a previously published investigation of blood metabolic profiles associated with the various ageing rate of fishes [19]. The research was focused on the analysis of metabolic compositions of fish muscle tissues for the identification of distinctive features between compared groups. A direct injection mass spectrometry (DIMS) approach was used in the study. Despite a large number of limitations (ion suppression, inability of isobars separation, etc.), until now DIMS has been a popular approach [20]. High throughput and reproducibility, wide metabolomic coverage (no loss of metabolites due to the application of any separation tools), and short analysis time are advantages of the DIMS method allow the improvement of the reliability and accuracy of the results of subsequent multivariate statistical analysis [20,21].

The largest number of identified metabolites belongs to lipids: a high level of storage lipids (tri- di- and monoacylglycerols, fatty acids, cholesterol) is found in salmonids. Accumulation of distinct phospholipids is detected for in each compared group. There are many of external and internal factors (environment, diet, feeding regime and digestion, etc.) that can influence the fatty acids' compositions in lipids [22,23]. For example, it was demonstrated that the level of muscle fatty acids composition of the same fish species depends on habitat-independent environmental factors [24,25]. Most likely the revealed differences in abundance of lipids in the compared fish species are the result of the effect of such factors. Salmonids are classified as "fatty" fish species because they have a large amount of storage lipids in muscle compared to other fish species [26,27].

There is very little information about the effects and possible mechanisms of action of lipids on biological processes which can be associated with aging. In some studies related to the aging research, an increase or decrease of the level of distinct lipids with age is noted. Unfortunately, the mechanism of this accumulation or loss of the lipids is not specified.

The intensification of glycogenolysis and glycolysis is the most probable cause of accumulation of metabolites of the "group of intermediates of sugar metabolism" (maltose, lactate, and pyruvate), medium and long-chain acylcarnitines, and the intermediates of the citric acid cycle (fumarate, malate, alpha-ketoglutarate, and citrate) (Figure 4, metabolites 33, 34, 39, 41, 42, 48, and 63), which are observed in the samples of rapid aging fish [28–33]. Activation of these processes with a simultaneous decline in the creatine and creatinine levels in salmonids species (Figure 4, metabolites 3 and 12) is probably due to the intensive swimming of fish during the migration for spawning [34]. However, it is possible that the accumulation of the intermediates of glucose is a result of any other factor or the combined effect of several factors. For example, mitochondrial dysfunction leads to similar changes: intracellular accumulation of intermediates of the citric acid cycle, intermediates of glucose metabolism, etc. [32,35–37].

Amino acids and biogenic amines, a high level of some of which was observed in negligible senescent and gradually aging species (Figure 4, metabolites 1, 8, 11, 13, and 14), exhibit a wide range of biological effects. Amino acids are one of the key elements of many cellular processes: differentiation and growth of skeletal muscles, osmoregulation, reproduction, immune response, and the precursors

of biologically active compounds [38]. They are involved in antioxidant protection (taurine and hypotaurine) and energy metabolism (alanine, valine, and leucine), enhance protein synthesis and inhibit proteolysis (leucine and valine) [39–42]. A number of studies have noted that an increase in the level of amino acids and biogenic amines leads to a decrease of the development and expression rate of age-related pathologies as well as an extension of the activity period of the musculoskeletal system in mammalia [43]. Most likely, the action of amino acids and biogenic amines in fish muscles is similar. However, the pathways for fish have not been established yet [38].

Based on the observations mentioned above, we can conclude that the capacity of antioxidant protection, the productivity of anabolic processes and, possibly, the effectiveness of energetic metabolism in skeletal muscle tissue samples obtained from negligible senescent and gradually aging species are higher in comparison with similar processes in skeletal muscle tissue samples related to rapid aging. A decrease in the effectiveness of these processes or their damage may lead to a loss of muscle mass and strength with aging [44].

4. Material and Methods

4.1. Muscle Sampling

The samples of young, ready-for-reproduction adults (all of them had visible developing gonads) were used in our work: the first group of pike (N: 12; an average mass of 1.2 ± 0.5 kg and body length—55 ± 7 cm) and sterlet (N: 12; 1.5 ± 0.3 kg; 70 ± 5 cm), the second group of zander (N: 10; 2.2 ± 1.1 kg; 50 ± 14 cm) and perch (N: 8; 0.13 ± 0.07 kg; 23 ± 3 cm), the third group—pink salmon (N: 10; 1.55 ± 0.45 g; 51 ± 3 cm) and chum salmon (N: 10; 3.1 ± 1.3 kg; 63 ± 7cm). The ratio of males to females for each species was approximately 1:1. The age of each fish was determined by analyzing the growth rings on the scales [45]. The salmon samples were obtained from fish caught near Sakhalin Island (Russia); all others were obtained from fish caught in the Uglich Reservoir (Russia) during September 2014 and May–June 2015 (collection permits: no. 69 2014 03 0722, no. 69 2015 03 0683, and no. 69 2016 03 0737, issued by the Federal Agency for Fisheries of the Russian Federation). The study was conducted in accordance with the Declaration of Helsinki.

Samples of muscles (about 0.1 g) were cut off from the spinal area. Visually, the samples did not contain any inclusions of other tissues. In order to better reflect the original metabolic state, the samples were immediately frozen and stored at $-80\ ^\circ$C before the analysis [46].

4.2. Extraction Method and Sample Preparation

The extraction methods used in this work were adapted from previously published investigations [47,48] with modifications. Frozen tissue samples were lyophilized overnight. Then, each sample was weighed, homogenized (Bandelin Sonopuls HD 2200, Sigma-Aldrich, St. Louis, MO, USA), divided into Eppendorf vials and extracted using 20 mL/g (dry mass) of solution ethanol-water (4:1), precooled to 4 $^\circ$C. After that, the suspension was maintained at 4 $^\circ$C for 60 min (incubation period) and strongly vortexed for 30 s (10 times), being placed on ice in between. All reagents were of analytical grade and were used without further purification. After centrifugation (15,000 g; 15 min; 4 $^\circ$C), the supernatant was collected, distributed into Eppendorf vials (Eppendorf, Hamburg, Germany) and stored at $-80\ ^\circ$C before analysis. Before mass spectrometry analysis to each aliquot (10 μL) of the supernatant, the fifty volumes of 90% methanol (Fluka, Munich, Germany) with 0.1% formic acid (Fluka, Munich, Germany) was added to obtain the analyzed solution [49].

4.3. Mass Spectrometry Analysis

The samples were analyzed using a hybrid quadrupole time-of-flight mass spectrometer (micrOTOFQ, Bruker Daltonics, Billerica, MA, USA) equipped with electrospray ionization (ESI) source. The mass spectrometer was set up for priority detection of ions with the mass-to-charge ratio (m/z) range from 80 to 1000 and mass accuracy up to 5 parts per million (ppm). ES Tuning

Mix (Agilent Technologies, Santa Clara, CA, USA) was used for calibration of the mass spectrometer. The spectra were recorded in the positive ion charge detection mode. The samples were injected into the ESI source using a glass syringe (Hamilton Bonaduz AG, Bonaduz, Switzerland) connected to a syringe injection pump (KD Scientific, Holliston, MA, USA). The flow rate of samples to the ionization source was 180 μL/h, and the samples were injected in a randomized order [49]. More detailed identification of the several selected metabolites was produced through ion fragmentation by collision-induced dissociation (CID) of the ions of interest (precursor ion). Ultra-pure nitrogen was used as collision gas. The fragmentation of the metabolites was performed at different collision energies (10 and 20 eV). The mass spectra were recorded using DataAnalysis version 3.4 (Bruker Daltonics, Germany) to summarize one-minute signals.

4.4. Data Analysis

Data analysis was used for the preliminary peak selection and recalibration of the spectra. The selection parameters were as follows: peak width—5, signal-to-noise ratio—2, relative and absolute threshold intensity—0.05% and 100 respectively. Alignment of mass spectrum peaks, removal of low-informative peaks, and data correction to address ionic inconsistency in samples were performed by using the self-made algorithm in Excel. Two peaks were considered to be related to the same metabolite if the mass difference did not exceed 0.05 Da. All peaks' intensity and area values were normalized by the internal standard (IS) losartan ($C_{22}H_{23}ClN_6O$, m/z = 423.169) concentration levels.

Analysis of acquired metabolite profiling data was performed by means of Principal Component Analysis (PCA) implemented in the software package ProfileAnalysis version 3.4 (Bruker Daltonics, Germany). Statistically significant differences between the study groups were evaluated using the Kruskal-Wallis H test implemented in the software package Statistica (StatSoft Inc., Tulsa, OK, USA).

4.5. Mass Spectra Peak Identification

The basic approach for identification of the selected peaks with clear isotope patterns consisted in searching of annotated metabolites, which had the closest m/z values to those detected in the spectra [50]. The following reference databases were used: Human Metabolome DataBase (HMDB) (http://www.hmbd.ca), METLIN (http://metlin.scripps.edu), and LIPID MAPS (www.lipidmaps.org). A mass tolerance window was 0.05 Da. Several additional steps were taken to minimize misidentification. Peaks of parental ion and possible adducts of suppositional metabolites in the spectra were found. Next, comparative analysis of isotope patterns of the metabolites or their possible adducts in the spectra with their theoretical isotope patterns was performed [50]. Theoretical isotope patterns for each of the metabolites and adducts were produced using Isotope Pattern Calculator (Bruker Daltonics, Germany). Tandem mass spectrometry (MS/MS) was applied for more specific identification of several metabolites. In this case, identification was performed by comparing the MS/MS spectra obtained at different collision energies in positive ionization modes with the reference MS/MS spectra from the public metabolite database (METLIN). A mass tolerance window, in this case, was 0.005 Da.

5. Conclusions

In summary, a wide range of metabolites that belong to different classes was detected in muscles of fish with different lifespan. Applications of metabolic profiling in combination with statistical analyses allowed to identify the group-specific features. The obtained results made it possible to suggest the biochemical pathways involving the identified metabolites and, perhaps, associated with the rate of aging. Utilization of these results may enhance our knowledge of aging processes, facilitate the development of new rational approaches to prevent or even delay age-associated alterations in muscle, and hence improve health lifespan.

Author Contributions: Conceptualization, D.L.M., M.V.M., P.G.L. and A.I.A.; methodology, D.L.M., M.V.M. and P.G.L.; software, D.L.M. and O.P.T. validation, D.L.M., K.V.Z. and M.V.M.; formal analysis, D.L.M. and O.P.T.; investigation, D.L.M., O.P.T., A.N.M., K.V.Z., K.V.N., V.I.N. and N.F.B.; resources, D.L.M., A.N.M., K.V.Z., K.V.N., V.I.N. and N.F.B.; data curation, D.L.M. and O.P.T.; writing—original draft preparation, D.L.M.; writing—review and editing, D.L.M., M.V.M. and P.G.L.; visualization, D.L.M.; supervision, D.L.M., M.V.M., P.G.L. and A.I.A.; project administration, D.L.M., M.V.M. and P.G.L.; funding acquisition, M.V.M., P.G.L. and A.I.A.

References

1. Finch, C.E.; Austad, S.N. History and prospects: Symposium on organisms with slow aging. *Exp. Gerontol.* **2001**, *36*, 593–597. [CrossRef]

2. Valdesalici, S.; Cellerino, A. Extremely short lifespan in the annual fish Nothobranchius furzeri. *Proc. R. Soc. B Biol. Sci.* **2003**, *270*, S189–S191. [CrossRef] [PubMed]

3. Finch, C. *Longevity, Senescence, and the Genome*; University of Chicago Press: Chicago, IL, USA, 1990.

4. Patnaik, B.K.; Mahapatro, N.; Jena, B.S. Ageing in fishes. *Gerontology* **1994**, *40*, 113–132. [CrossRef]

5. Craig, C.; Kipling, J.F. Reproduction effort versus the environment; case histories of Windermere perch, *Perca fluviatilis* L., and pike, *Esox lucius* L. *J. Fish Biol.* **1983**, *22*, 713–727. [CrossRef]

6. Kirczuk, L.; Domagała, J.; Pilecka-Rapacz, M. Annual Developmental Cycle of Gonads of European Perch Females (*Perca fluviatilis* L.) from Natural Sites and a Canal Carrying Post-cooling Water from the Dolna Odra Power Plant (NW Poland). *Folia Biol.* **2015**, *63*, 85–93. [CrossRef]

7. Gorbunova, V.; Seluanov, A.; Zhang, Z.; Gladyshev, V.N.; Vijg, J. Comparative genetics of longevity and cancer: Insights from long-lived rodents. *Nat. Rev. Genet.* **2014**, *15*, 531–540. [CrossRef] [PubMed]

8. Selman, C.; Withers, D.J. Mammalian models of extended healthy lifespan. *Philos. Trans. R. Soc. Lond. B. Biol. Sci.* **2011**, *366*, 99–107. [CrossRef] [PubMed]

9. Moskalev, A.A.; Pasyukova, E.G. From theories of aging to anti-aging interventions. *Front. Genet.* **2014**, *5*, 276. [CrossRef]

10. Rosenberg, I.H. Sarcopenia: Origins and clinical relevance. *Clin. Geriatr. Med.* **2011**, *27*, 337–339. [CrossRef]

11. Baumgartner, R.N.; Koehler, K.M.; Gallagher, D.; Romero, L.; Heymsfield, S.B.; Ross, R.R.; Garry, P.J.; Lindeman, R.D. Epidemiology of sarcopenia among the elderly in New Mexico. *Am. J. Epidemiol.* **1998**, *147*, 755–763. [CrossRef] [PubMed]

12. Melton, L.J.; Khosla, S.; Riggs, B.L. Epidemiology of sarcopenia. *Mayo Clin. Proc.* **2000**, *75*, S10–S13.

13. Jeromson, S.; Gallagher, I.J.; Galloway, S.D.R.; Hamilton, D.L. Omega-3 fatty acids and skeletal muscle health. *Mar. Drugs* **2015**, *13*, 6977–7004. [CrossRef] [PubMed]

14. Payne, B.A.I.; Chinnery, P.F. Mitochondrial dysfunction in aging: Much progress but many unresolved questions. *Biochim. Biophys. Acta Bioenerg.* **2015**, *1847*, 1347–1353. [CrossRef]

15. Deberardinis, R.J.; Thompson, C.B. Cellular metabolism and disease: What do metabolic outliers teach us? *Cell* **2012**, *148*, 1132–1144. [CrossRef] [PubMed]

16. Dunn, W.B.; Erban, A.; Weber, R.J.M.; Creek, D.J.; Brown, M.; Breitling, R.; Hankemeier, T.; Goodacre, R.; Neumann, S.; Kopka, J.; et al. Mass appeal: Metabolite identification in mass spectrometry-focused untargeted metabolomics. *Metabolomics* **2013**, *9*, 44–66. [CrossRef]

17. Kahwati, L.; Jacobs, S.; Kane, H.; Lewis, M.; Viswanathan, M.; Golin, C.E. Using qualitative comparative analysis in a systematic review of a complex intervention. *Syst. Rev.* **2016**, *5*, 82. [CrossRef] [PubMed]

18. Gilbert, M.J.H.; Zerulla, T.C.; Tierney, K.B. Zebrafish (Danio rerio) as a model for the study of aging and exercise: Physical ability and trainability decreases with age. *Exp. Gerontol.* **2014**, *50*, 106–113. [CrossRef]

19. Trifonova, O.P.; Maslov, D.L.; Mikhailov, A.N.; Zolotarev, K.V.; Nakhod, K.V.; Nakhod, V.I.; Belyaeva, N.F.; Mikhailova, M.V.; Lokhov, P.G.; Archakov, A.I.; et al. Comparative Analysis of the Blood Plasma Metabolome of Negligible, Gradual and Rapidly Ageing Fishes. *Fishes* **2018**, *3*, 46. [CrossRef]

20. Cajka, T.; Danhelova, H.; Vavrecka, A.; Riddellova, K.; Kocourek, V.; Vacha, F.; Hajslova, J. Evaluation of direct analysis in real time ionization–mass spectrometry (DART–MS) in fish metabolomics aimed to assess the response to dietary supplementation. *Talanta* **2013**, *115*, 263–270. [CrossRef] [PubMed]

21. Dettmer, K.; Aronov, P.A.; Hammock, B.D. Mass Spectrometry-Based Metabolomics. *Mass Spectrom. Rev.* **2007**, *26*, 51–78. [CrossRef]

22. Sérot, T.; Gandemer, G.; Demaimay, M. Lipid and fatty acid compositions of muscle from farmed and wild adult turbot. *Aquac. Int.* **1998**, *6*, 331–343. [CrossRef]

23. Megdal, P.A.; Craft, N.A.; Handelman, G.J. A simplified method to distinguish farmed (Salmo salar) from wild salmon: Fatty acid ratios versus astaxanthin chiral isomers. *Lipids* **2009**, *44*, 569–576. [CrossRef] [PubMed]

24. Özogul, Y.; Özogul, F. Fatty acid profiles of commercially important fish species from the Mediterranean, Aegean and Black Seas. *Food Chem.* **2007**, *100*, 1634–1638. [CrossRef]

25. Özogul, Y.; Özogul, F.; Alagoz, S. Fatty acid profiles and fat contents of commercially important seawater and freshwater fish species of Turkey: A comparative study. *Food Chem.* **2007**, *103*, 217–223. [CrossRef]

26. Jobling, M.; Johansen, S.J.S.; Foshaug, H.; Burkow, I.C.; Jørgensen, E.H. Lipid dynamics in anadromous Arctic charr, Salvelinus alpinus (L.): Seasonal variations in lipid storage depots and lipid class composition. *Fish Physiol. Biochem.* **1998**, *18*, 225–240. [CrossRef]

27. Josrgensen, E.H.; Johansen, S.J.S.; Jobling, M. Seasonal patterns of growth, lipid deposition and lipid depletion in anadromous Arctic charr. *J. Fish Biol.* **1997**, *51*, 312–326. [CrossRef]

28. Hiatt, W.R.; Regensteiner, J.G.; Wolfel, E.E.; Ruff, L.; Brass, E.P. Carnitine and acylcarnitine metabolism during exercise in humans. Dependence on skeletal muscle metabolic state. *J. Clin. Investig.* **1989**, *84*, 1167–1173. [CrossRef]

29. Sabatine, M.S.; Liu, E.; Morrow, D.A.; Heller, E.; McCarroll, R.; Wiegand, R.; Berriz, G.F.; Roth, F.P.; Gerszten, R.E. Metabolomic Identification of Novel Biomarkers of Myocardial Ischemia. *Circulation* **2005**, *112*, 3868–3875. [CrossRef]

30. Koves, T.R.; Ussher, J.R.; Noland, R.C.; Slentz, D.; Mosedale, M.; Ilkayeva, O.; Bain, J.; Stevens, R.; Dyck, J.R.B.; Newgard, C.B.; et al. Mitochondrial overload and incomplete fatty acid oxidation contribute to skeletal muscle insulin resistance. *Cell Metab.* **2008**, *7*, 45–56. [CrossRef]

31. Lehmann, R.; Zhao, X.; Weigert, C.; Simon, P.; Fehrenbach, E.; Fritsche, J.; Machann, J.; Schick, F.; Wang, J.; Hoene, M.; et al. Medium chain acylcarnitines dominate the metabolite pattern in humans under moderate intensity exercise and support lipid oxidation. *PLoS ONE* **2010**, *5*, e11519. [CrossRef] [PubMed]

32. Houtkooper, R.H.; Argmann, C.; Houten, S.M.; Cantó, C.; Jeninga, E.H.; Andreux, P.A.; Thomas, C.; Doenlen, R.; Schoonjans, K.; Auwerx, J. The metabolic footprint of aging in mice. *Sci. Rep.* **2011**, *1*, 134. [CrossRef]

33. Gumucio, J.P.; Mendias, C.L. Atrogin-1, MuRF-1, and sarcopenia. *Endocrine* **2013**, *43*, 12–21. [CrossRef] [PubMed]

34. McCommis, K.S.; Finck, B.N. Mitochondrial pyruvate transport: A historical perspective and future research directions. *Biochem. J.* **2015**, *466*, 443–454. [CrossRef]

35. Darras, B.T.; Friedman, N.R. Metabolic myopathies: A clinical approach; part I. *Pediatr. Neurol.* **2000**, *22*, 87–97. [CrossRef]

36. Baraibar, M.A.; Hyzewicz, J.; Rogowska-Wrzesinska, A.; Bulteau, A.-L.; Prip-Buus, C.; Butler-Browne, G.; Friguet, B. Impaired energy metabolism of senescent muscle satellite cells is associated with oxidative modifications of glycolytic enzymes. *Aging* **2016**, *8*, 3375–3389. [CrossRef]

37. Wan, Q.-L.; Shi, X.; Liu, J.; Ding, A.-J.; Pu, Y.-Z.; Li, Z.; Wu, G.-S.; Luo, H.-R. Metabolomic signature associated with reproduction-regulated aging in Caenorhabditis elegans. *Aging* **2017**, *9*, 447–474. [CrossRef] [PubMed]

38. Li, P.; Mai, K.; Trushenski, J.; Wu, G. New developments in fish amino acid nutrition: Towards functional and environmentally oriented aquafeeds. *Amino Acids* **2009**, *37*, 43–53. [CrossRef] [PubMed]

39. Kimball, S.R.; Jefferson, L.S. Signaling pathways and molecular mechanisms through which branched-chain amino acids mediate translational control of protein synthesis. *J. Nutr.* **2006**, *136*, 227S–231S. [CrossRef] [PubMed]

40. Newgard, C.B.; An, J.; Bain, J.R.; Muehlbauer, M.J.; Stevens, R.D.; Lien, L.F.; Haqq, A.M.; Shah, S.H.; Arlotto, M.; Slentz, C.A.; et al. A branched-chain amino acid-related metabolic signature that differentiates obese and lean humans and contributes to insulin resistance. *Cell Metab.* **2009**, *9*, 311–326. [CrossRef] [PubMed]

41. Miyazaki, T.; Honda, A.; Ikegami, T.; Matsuzaki, Y. The role of taurine on skeletal muscle cell differentiation. *Adv. Exp. Med. Biol.* **2013**, *776*, 321–328. [PubMed]

42. Spriet, L.L.; Whitfield, J. Taurine and skeletal muscle function. *Curr. Opin. Clin. Nutr. Metab. Care* **2015**, *18*, 96–101. [CrossRef]

43. Minois, N. Molecular basis of the "anti-aging" effect of spermidine and other natural polyamines—A mini-review. *Gerontology* **2014**, *60*, 319–326. [CrossRef] [PubMed]

44. Glover, E.I.; Phillips, S.M.; Oates, B.R.; Tang, J.E.; Tarnopolsky, M.A.; Selby, A.; Smith, K.; Rennie, M.J. Immobilization induces anabolic resistance in human myofibrillar protein synthesis with low and high dose amino acid infusion. *J. Physiol.* **2008**, *586*, 6049–6061. [CrossRef] [PubMed]

45. Tesch, F.W. Age and Growth. In *Methods for Assessment of Fish Production in Fresh Waters*; Ricker, W.E., Ed.; Blackwell Sci. Pub.: Oxford, UK, 1968; pp. 93–123.

46. Rammouz, R.E.; Létisse, F.; Durand, S.; Portais, J.C.; Moussa, Z.W.; Fernandez, X. Analysis of skeletal muscle metabolome: Evaluation of extraction methods for targeted metabolite quantification using liquid chromatography tandem mass spectrometry. *Anal. Biochem.* **2010**, *398*, 169–177. [CrossRef] [PubMed]

47. Van Scoy, A.R.; Yu Lin, C.; Anderson, B.S.; Philips, B.M.; Martin, M.J.; McCall, J.; Todd, C.R.; Crane, D.; Sowby, M.L.; Viant, M.R.; et al. Metabolic responses produced by crude versus dispersed oil in Chinook salmon pre-smolts via NMR-based metabolomics. *Ecotoxicol. Environ. Saf.* **2010**, *73*, 710–717. [CrossRef] [PubMed]

48. Lin, C.Y.; Wu, H.; Tjeerdema, R.S.; Viant, M.R. Evaluation of metabolite extraction strategies from tissue samples using NMR metabolomics. *Metabolomics* **2007**, *3*, 55–67. [CrossRef]

49. Lokhov, P.G.; Kharybin, O.N.; Archakov, A.I. Diagnosis of lung cancer based on direct-infusion electrospray mass spectrometry of blood plasma metabolites. *Int. J. Mass Spectrom.* **2012**, *309*, 200–205. [CrossRef]

50. Lynn, K.-S.; Cheng, M.-L.; Chen, Y.-R.; Hsu, C.; Chen, A.; Lih, T.M.; Chang, H.-Y.; Huang, C.; Shiao, M.-S.; Pan, W.-H.; et al. Metabolite identification for mass spectrometry-based metabolomics using multiple types of correlated ion information. *Anal. Chem.* **2015**, *87*, 2143–2151. [CrossRef]